ACS APPLIED MATERIALS & INTERFACES

Letter

www.acsami.org

Multifunctional Protein-Enabled Patterning on Arrayed Ferroelectric Materials

M. Hnilova,[†,‡,§] X. Liu,[§,‡] E. Yuca,[†,⊥,‡] C. Jia,[†] B. Wilson,[†,§] A. Y. Karatas,[#] C. Gresswell,[†] F. Ohuchi,[§] K. Kitamura,[∥] and C. Tamerler*[,†,§]

[†]GEMSEC, Genetically Engineered Materials Science and Engineering Center, and [§]Department of Material Science and Engineering, University of Washington, Seattle, Washington 98195, United States

[⊥]Department of Biology, Yildiz Technical University, 34210, Istanbul, Turkey

[#]Department of Molecular Biology and Genetics, Istanbul Technical University, 34220, Istanbul, Turkey

[∥]Optical & Electronic Materials Unit, National Institute for Materials Science, Tsukuba, Ibaraki 305-0044, Japan

Supporting Information

ABSTRACT: This study demonstrates a biological route to programming well-defined protein-inorganic interfaces with an arrayed geometry via modular peptide tag technology. To illustrate this concept, we designed a model multifunctional fusion protein, which simultaneously displays a maltose-binding protein (MBP), a green fluorescence protein (GFPuv) and an inorganic-binding peptide (AgBP2C). The fused combinatorially selected AgBP2C tag controls and site-directs the multifunctional fusion protein to immobilize on silver nanoparticle arrays that are fabricated on specific domain surfaces of ferroelectric $LiNbO_3$ via photochemical deposition and in situ synthesis. Our combined peptide-assisted biological and ferroelectric lithography approach offers modular design and versatility in tailoring surface reactivity for fabrication of nanoscale devices in environmentally benign conditions.

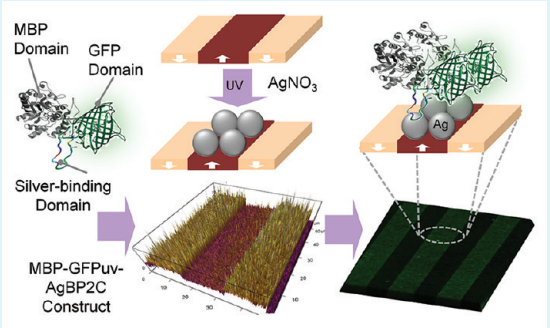

KEYWORDS: *heterofunctional proteins, hierarchical assemblies, ferroelectric $LiNbO_3$ substrate, photochemical deposition, protein microarrays, biological-material interface*

The ability to control hierarchical assemblies of hybrid nanostructures and biological building blocks is essential for a wide range of practical biotechnological and diagnostics applications, as well as in fabrication of biomedical and biosensing devices.[1−5] One of the main challenges is the development of novel fabrication techniques that are flexible and low-cost but also able to precisely control layer-by-layer self-assembly at a molecular level and thus provide control over the biological and inorganic interfaces. The desired fabrication and processing conditions would ideally be environmentally benign and biologically compatible. In the past few decades, several notable deposition methods have been developed to fabricate multilayered molecular solid films, among these techniques are atomic layer,[6] Langmuir−Blodgett,[7] and multilayer-deposition based on the use of various polymeric materials[8] and self-assembled monolayers (SAMs).[9] Although used in many successful surface functionalization applications, these conventional deposition techniques and processes may also exhibit significant shortcomings.[2−4,10] For example, the common thiol and silane SAMs bind to either noble metals or oxides, respectively, forming densely packed films onto a narrow range of solid surfaces.[4,9,10] A number of SAMs molecules, especially silanes, also require complex or nonbiocompatible reaction conditions.[10,11] Additionally, the biocompability associated with some of the SAMs components still remains in question limiting their wide range use in biotechnological and biomedical applications.[11] In contrast, Langmuir−Blodgett films consisting of amphiphiles, assemble without the necessity of chemical bonding by mimicking a cell membrane.[4,7] Although the Langmuir−Blodgett technique allows control over film density and thickness, the expensive instrumentation, long fabrication periods, film instability, challenging optimization and transition between materials are limiting factors for practical applications in biotechnology.[4,11]

In recent years, the study of biology-based concepts that can provide control over the assembly process and their interfaces has interested many researchers. An alternative immobilization and deposition technique has emerged using biocombinatorially selected inorganic-binding peptides.[11−14] These peptides bind with high affinity to their respective materials, with dissociation constant (K_D) values in the μM to nM range, while also exhibiting desired material selectivity.[11−15] Several inorganic-binding peptides have already been shown to form densely packed monolayers, which is an advantage in surface engineering

Received: January 31, 2012
Accepted: March 29, 2012
Published: March 29, 2012

and modification applications. Another unique feature of these peptides is their relatively simple conjugation protocol with complex proteins via site-directed genetic recombination. Our group and others have pioneered the utility of the inorganic-binding peptides in association with various fusion partners, such as proteins or peptides, building heterofunctional units for a variety of directed self-assembly applications.[10,12,16−19] In previous reports, we showed that specific inorganic-binding peptide tags provide an effective and viable strategy for versatile and site-directed protein immobilization on flat solid surfaces.[10,11,14,20] These tags offer significant advantages compared to less controlled immobilization techniques utilizing nonspecific interactions of side groups such as histidine and cysteine-tagged amino acids with metallic surfaces, e.g., gold, silver, and nickel.[21−24]

In the present study, we demonstrate the efficient combination of a bioenabled route with a unique lithographic technique[25−27] resulting in protein immobilization with a programmable interface on silver nanoparticles (AgNP) patterned on functional ferroelectric $LiNbO_3$ substrates. Specifically, as a material-specific biolinker, we use a combinatorially selected silver-binding peptide fused to a maltose-binding protein and a green fluorescent protein so as to produce a single-, multifunctional-protein construct. We utilized this multifunctional protein construct in peptide-mediated protein immobilization onto desired locations of AgNP patterns on $LiNbO_3$ domain surfaces. Our combined peptide-assisted biological and ferroelectric lithography method offers modular design and versatility in tailoring surface reactivity for fabrication of nanoscale devices with potential impact on diverse fields of medicine and technology.

To obtain high-affinity silver-binding peptides (AgBPs), we screened the FliTrx bacterial surface library[28] using modified combinatorial selection procedures.[29] We selected and sequenced 50 unique clones from a biocombinatorially enriched population to determine the amino acid sequence of their randomized peptide insertions. Additionally, we tested the binding affinities of individual peptides using fluorescence microscopy,[11,29] a semi-quantitative technique that allowed us to identify several AgBPs exhibiting the desired binding characteristics toward Ag when they were displayed by bacterial cells as FliTrx fusion surface proteins. The cell adhesion capabilities of isolated bacterial clones displaying high-affinity (AgBP1C and AgBP2C) and low-affinity (AgBP30) FliTrx fusion surface proteins to Ag surfaces are demonstrated in Figure S1 in the Supporting Information. As evidenced in Figure S1, the clone expressing AgBP2C sequence displays a very high binding affinity and material selectivity to Ag surfaces. Furthermore, we compared the observed amino acid composition among strong and weak binder groups with the unpanned library and calculated the relative amino acid abundances. We found that Asp, Cys, Lys, Gln, and Tyr were overexpressed, and His, Gly, Trp, and Val under-expressed among our strong binder sequences (Figure 1a). The overexpression of Cys would be expected since the thiol group has an affinity to metallic surfaces.[30,31]

Following the biopanning selection, we verified the binding characteristics of chemically synthesized AgBP1C and AgBP2C peptides onto an Ag surface using an established surface plasmon resonance (SPR) technique. Raw SPR kinetic data of tested AgBP peptides (0.66 μM) on Ag surfaces were fitted by least-squares regression to a modified Langmuir adsorption model reported previously by our group (Figure 1b).[32] Using the Langmuir adsorption binding model, we calculated kinetic binding parameters, apparent binding constant (k_{obs}) and

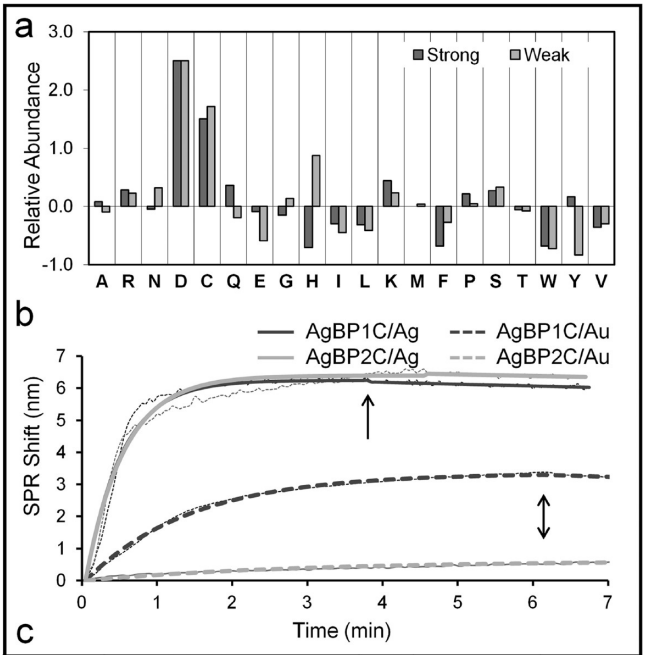

Name	Peptide Sequence	pI	k_{obs} (s^{-1})	Adhered mass (ng/cm^2)
AgBP1C	CGPTGIFKSARAMRNGPC	9.7	0.044±0.013	162±10
AgBP2C	CGPEQLGVRKELRGVGPC	8.1	0.042±0.013	150±20

Figure 1. Biocombinatorial selection and binding characterization of AgBP peptides displayed on host. (a) Relative amino acid abundance in strong and weak binder group selected from AgBP biopanning experiment. (b) SPR binding sensograms fitted with Langmuir adsorption model recorded for synthesized AgBP1C and AgBP2C peptides on silver and gold surface. (c) Table of calculated binding coefficients (k_{obs} and adhered peptide mass) for AgBP1C and AgBP2C on silver surface. The arrows indicate the start of the desorption process.

surface coverage following the desorption process after the washing step. The respective adhered peptide masses after the desorption step were calculated based on the method provided in the literature.[33] The observed k_{obs} and adhered peptide mass detected for both AgBP peptides at the 0.66 μM concentration tested are within the range observed for combinatorially selected peptides (Figure 1c).[29,32,34−36] As further evidenced in SPR sensorgrams (Figure 1b), the tested AgBP2C peptide exhibited significant material recognition and bound preferentially to the Ag surface compared to binding on the Au surface. Specifically, at the 1.33 μM AgBP2C peptide concentration tested, we detected only negligible peptide adhesion to Au surface, corresponding approximately to more than a 10-fold reduction of adhered peptide mass compared to binding to the Ag surface. The enhanced material selectivity and high binding affinity of chemically synthesized AgBP2C sequence is consistent with observed specific binding behavior of combinatorially selected clones expressing the same sequence (see Figure S1 in the Supporting Information). This finding suggests that the AgBP2C sequence is selective to silver, an important feature for potential future surface functionalization schemes of our protein fusion system.

On the basis of our hypothesis and previous findings, we predicted that the display of a specific inorganic-binding peptide tag in the fusion protein constructs would increase the protein affinity, as well as protein molecular organization and

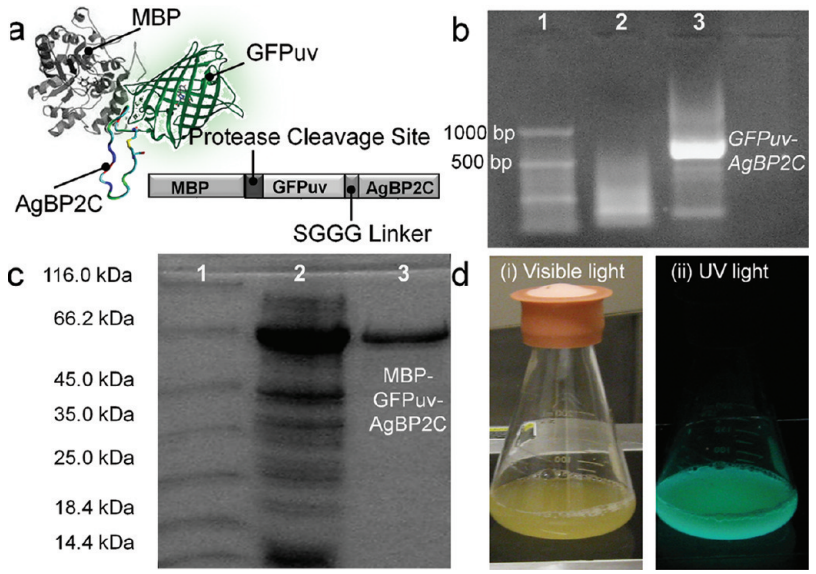

Figure 2. Construction of heterofunctional protein. (a) Schematic design of MBP-GFPuv-AgBP2C fusion protein. (b) DNA fragment encoding the fusion protein. Lane 1, O'Range Ruler 50 bp DNA ladder (Fermentas International Inc.); lane 2, control; lane 3, GFPuv-AgBP2C encoding DNA fragment. (c) SDS-PAGE analysis of protein samples. Lane 1, molecular weight standard (Fermentas International Inc.); lane 2, induced bacterial cells expressing MBP-GFPuv-AgBP2C protein; lane 3, purified MBP-GFPuv-AgBP2C. (d) Bacterial culture expressing MBP-GFPuv-AgBP2C fusion protein under (i) visible and (ii) UV light.

orientation on the surface. To test this prediction, we engineered and designed a model heterofunctional fusion protein simultaneously displaying three different functionalities; maltose binding protein (MBP), green fluorescent protein (GFPuv), and Ag binding peptide (AgBP2C) domains. We rationally selected the MBP fusion based upon ease of genetic manipulation, as well as its high expression protein yield in bacterial cells and easy purification. Additionally, the lack of cysteine in the MBP component prevents the sulfide-induced nonspecific protein interactions with metallic surface, and eliminates various elusive issues regarding nonspecific interactions. The second fusion partner, fluorescently active GFPuv protein, was chosen to visualize the model fusion protein immobilized on defined locations on silver surfaces. We separated the two functional domains, the silver-binding AgBP2C tag from the fluorescent GFPuv protein, by a flexible (SGGG) spacer, which itself is separated from the MBP protein by several amino acids encoded by the polylinker contained in the pMAL-c4x expression vector (Figure 2a). In our design, the fused combinatorially selected AgBP2C was utilized to control and site-direct the immobilization of multifunctional fusion protein on silver surfaces, whereas the MBP and GFP components were utilized in the robust purification scheme for efficient protein recovery and effective detection of surface-bound fusion protein.

The bacterial cell culture containing the heterofunctional MBP-GFPuv-AgBP2C plasmid construct (Figure 2b,c), produced heterofunctional proteins that were isolated using strategies explained in Supporting Information, emitted fluorescent light under ultraviolet radiation as a result of the expression of heterofunctional MBP-GFPuv-AgBP2C protein (Figure 2d). The purity and molecular weight of the heterofunctional MBP-GFPuv-AgBP2C protein was verified using SDS–PAGE and a single band was observed at the location corresponding to theoretical molecular weight of the heterofunctional construct, 71.903 kDa. Furthermore, as evidenced by surface plasmon resonance, the heterofunctional MBP-GFPuv-AgBP2C fusion protein immobilized on the silver surface with considerably higher affinity and density compared to MBP-GFPuv protein at the same protein concentration (0.1 μM) tested (see Figure S4 in the Supporting Information). These results confirmed that the heterofunctional MBP-GFPuv-AgBP2C fusion protein conserved the desired functionalities, fluorescence emission and silver-binding activity.

To further demonstrate the silver-binding capacity of AgBP2C peptide tag, we fabricated protein arrays on silver surfaces in a single reaction step by taking advantage of the high efficiency of conventional microcontact printing (μCP). As demonstrated in Figure 3, fluorescence microscopy data revealed the enhanced efficiency of MBP-GFPuv-AgBP2C fusion protein compared to MBP-GFPuv alone in the fabrication process of protein arrays. It is apparent that MBP-GFPuv-AgBP2C proteins assemble on silver surface forming high molecular packing density and patterning efficiency as evidenced by bright, well-defined protein patterns (Figure 3b), that resulted in approximately 8-fold enhancement of the detected fluorescence emission (Figure 3c). These data suggest that the specific AgBP2C tag present in MBP-GFPuv-AgBP2C fusion protein indeed controls and directs the immobilization of fusion proteins on the silver surface.

We next demonstrate the protein micropatterning on spatially distributed arrays of AgNPs by performing bioenabled immobilization on photochemically produced AgNPs on $LiNbO_3$ substrates. $LiNbO_3$ is a widely known ferroelectric material benefiting from large polarization (P_s) existing only along the crystallographic *c*-axis (Figure 4a). Polarization orientations can be manipulated by an external electric field (Figure 4b), which give rise to many applications based on ferroelectric materials.[37,38] Inspired by the concept that spontaneous polarization (P_s) in ferroelectric materials has a strong effect on surface reactivity we combined the polarization inversion with polarization-dependent photochemical reactions and fabricated AgNPs micropatterns on the $LiNbO_3$ surface. Specifically, the periodically poled $LiNbO_3$ of congruent composition, PPLN (Swing Ltd. Japan), diced in 3×5 mm^2 with a thickness of 0.5 mm was used as the deposition

dx.doi.org/10.1021/am300177t | ACS Appl. Mater. Interfaces 2012, 4, 1865–1871

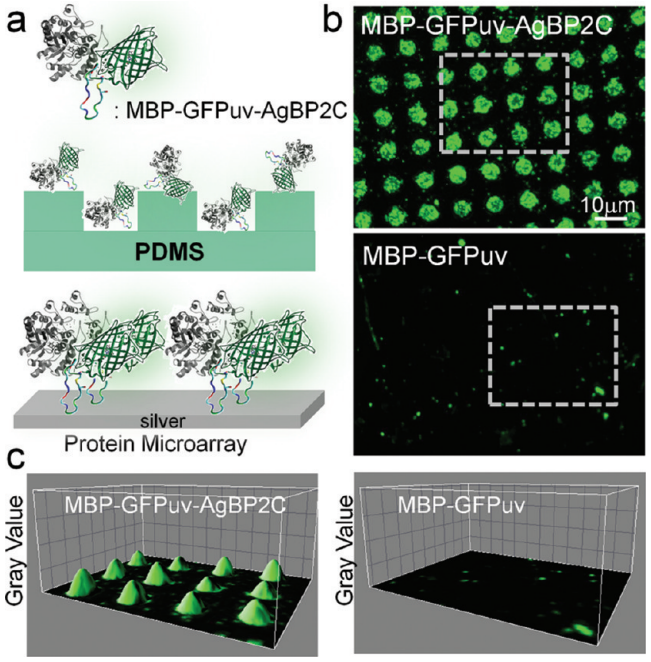

Figure 3. Protein microarrays on flat silver surface via microcontact printing technique. (a) Schematics of microcontact printing. (b) Representative fluorescence images of protein arrays fabricated by microcontact printing of 8 μM MBP-GFPuv and MBP-GFPuv-AgBP2C proteins. (c) Respective 3D surface plots of highlighted regions from fluorescence images generated by ImageJ imaging software shown in b.

substrate. Domain structures exhibiting antiparallel polarization along their *c*-axis were fabricated following a photolithographic step. Before deposition, the surface topography of PPLN substrate was examined by atomic force microscope (AFM). The bare substrate was observed as a flat surface by AFM (roughness 1−3 nm) with no surface features associated with the domain structure (Figure 4c). Domain structure was next visualized by phase image of piezoresponse force microscope (PFM) and a periodically poled domain pattern with 180° domains in a width of ∼12 μm was identified (Figure 4c). The contrast variation in the PFM phase image allows the identification of domain polarity: dark contrast indicates "+*c* domains", whereas bright contrast corresponds to "−*c* domains". Domain specific Ag deposition can be facilitated by the strong photovoltaic effect[26,39] of the $LiNbO_3$ crystals. Next we conduct the photochemical deposition by placing $AgNO_3$ aqueous solution over the substrate surface under UV irradiation. The AgNPs pattern fabricated by the photochemical deposition was confirmed by non-contact AFM. Figure 4c-d shows the typical AgNPs pattern where the particle diameter ranges from 30 to 50 nm resulting from 20 minutes of UV irradiation. An additional advantage of using photochemically fabricated AgNP patterned surfaces is that the Raman intensity of adsorbed molecules can be enhanced by surface plasmonic resonance effect of homogeneously distributed and densely packed AgNPs with well-controlled particle size.

By taking advantage of the multifunctional modalities contained in the designed MBP-GFPuv-AgBP2C protein, we next fabricated

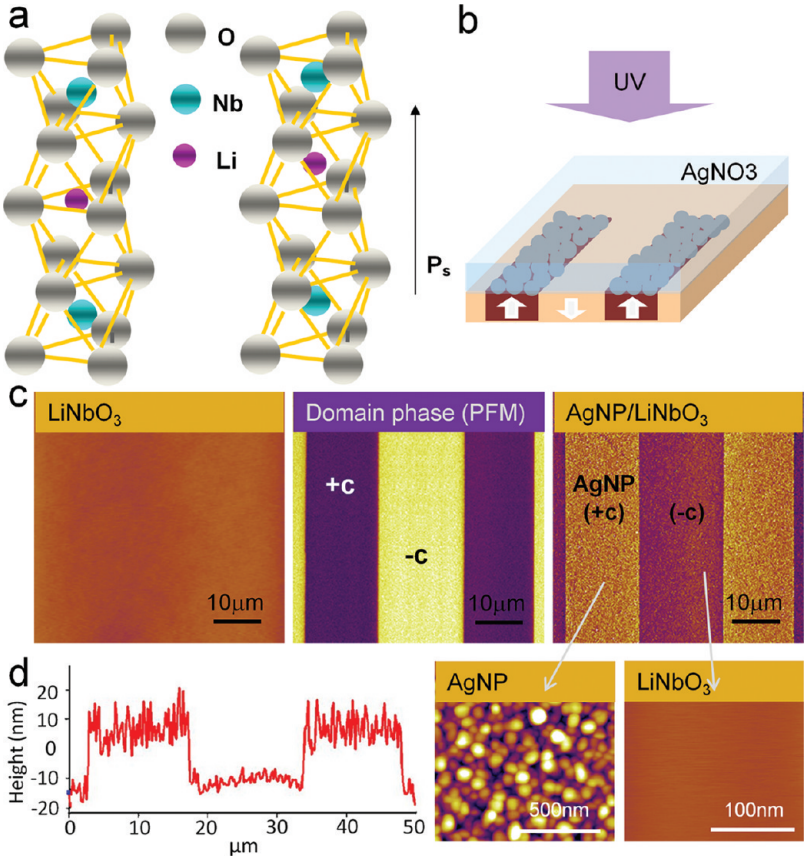

Figure 4. (a) Crystallographic structure of $LiNbO_3$. (b) Schematic of photochemical deposition of AgNPs. (c) (left) Topographic image of the PPLN substrate before deposition, (middle) corresponding PFM phase image of the PPLN substrate, (right) topographic image of the same substrate after deposition. (d) Height profile and higher-resolution topographic image illustrating the morphology of deposited AgNPs and unmodified PPLN surface.

dx.doi.org/10.1021/am300177t | *ACS Appl. Mater. Interfaces* 2012, 4, 1865−1871

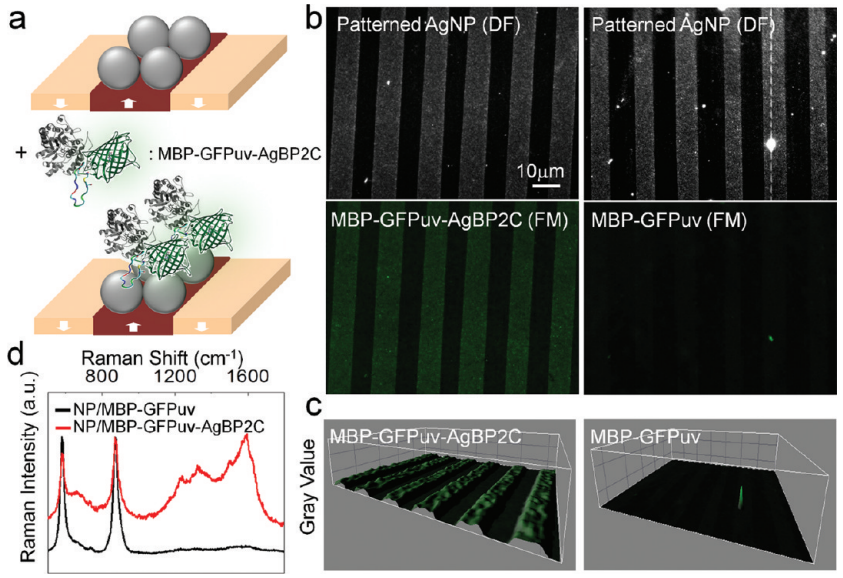

Figure 5. Protein array on AgNP patterned ferroelectric surface. (a) Schematics of targeted protein immobilization on AgNP pattern generated by photochemical deposition on $LiNbO_3$. (b) Representative fluorescence and dark field images of 20 μM MBP-GFPuv and MBP-GFPuv-AgBP2C proteins immobilized on AgNP pattern. (c) Corresponding 3D surface plots of fluorescence images generated by ImageJ imaging software. (d) Comparison of SERS spectra taken from AgNP pattern with MBP-GFPuv-AgBP2C and MBP-GFPuv protein.

protein arrays on the produced AgNPs patterns that are located on the PPLN substrate (Figure 5a). The fluorescent microscopy data shown in Figure 5b-c confirms the high-affinity and material-selective self-assembly of MBP-GFPuv-AgBP2C fusion proteins onto AgNP array regions resulting in fabrication of spatially controllable, multilayered protein arrays. In contrast MBP-GFPuv protein did not produce comparable protein arrays and rather resulted in random, nonspecific immobilization of MBP onto both solid surfaces (Figure 5b).

Additionally, we employed the surface-enhanced Raman scattering (SERS) in order to confirm the presence of MBP-GFPuv-AgBP2C protein adsorbed on the optically active AgNPs arrays patterned on the PPLN substrate. Figure 5d shows the observed SERS spectra of immobilized MBP-GFPuv-AgBP2C in comparison to its wild type MBP-GFPuv counterpart averaged from multiple analyzed locations. The detected SERS bands in the MBP-GFPuv-AgBP2C sample correspond to asymmetric NH_3^+ bending vibration (1626 cm^{-1} in lysine); NH_2 bending vibration (1593 and 1586 cm^{-1} in glutamine); C−C stretching and C−H bending vibrations (1517 cm^{-1} in tyrosine aromatic side group); asymmetric CH_3 bending vibration (1472 cm^{-1}); imidazole group and C−H bending vibration (1340 and 1336 cm^{-1} in tryptophan); C−H bending and C−C stretching vibrations (1245 cm^{-1} in tryptophan); and C−O and C−C stretching vibrations (1240 cm^{-1} in tyrosine) present in the heterofunctional protein unit.[17,40] Similarly to observed fluorescence microscopy results, MBP-GFPuv protein sample did not generate any detectable SERS bands in these regions under identical experimental condition suggesting that only a few molecules may have been bound to the AgNP surface. The two detected peaks at 581 and 872 nm are associated with the underlying PPLN substrate.[41] In summary, the observed SERS data confirms the enhanced self-assembly of MBP-GFPuv-AgBP2C fusion proteins through controlled orientation onto AgNP array regions provided by AgBP2C tag.

The described combined micropatterning procedure is highly modular and can be extended to immobilize a variety of other inorganic nanoentities. As shown in Figure S6 in the Supporting Information, the well-defined patterns of streptavidin-modified QDots immobilized on top of the AgNPs patterns of PPLN substrate were produced via specific AgBP2C peptide tag functionalized with biotin and biotin-streptavidin interactions. The data suggest that AgBP2C peptide linkers can be used as biological surface functionalization molecules exerting their control over the interface at the molecular level.

Overall, we report a unique combination of bioenabled protein self-assembly and ferroelectric lithography (top-down and bottom-up) techniques for fabrication of well-organized protein microarrays with genetically programmable design. Specifically, we engineered a model heterofunctional protein unit containing three structural and functional components, MBP protein, fluorescently active GFPuv protein and highly specific AgBP2C peptide tag selected using a FliTrx combinatorial peptide library. The AgBP2C peptide tag serves to enhance the binding affinity of the heterofunctional MBP-GFPuv-AgBP2C protein construct onto various silver surfaces through its exceptional molecular recognition and self-assembly characteristics. Moreover, the AgBP2C motif controlled and directed the fusion protein immobilization to AgNP patterns generated by photochemical deposition on ferroelectric $LiNbO_3$ and in situ synthesis. The oriented immobilization of a multifunctional fusion protein on arrayed silver nanoparticles offers extensive opportunities to engineer responsive biosensing platforms based on plasmonic and photonic phenomenon. Described heterofunctional fusion protein construct as well as the proposed modular concept can be utilized in advanced studies that require or benefit from directed organization of biomolecules on the surface (e.g., Raman spectroscopy, SERS and FRET/RET techniques). In such application, the silver-binding peptide tag can offer the material selectivity as well as proximity and alignment control between the desired functional biomolecule and material interfaces.

We note that the reported combined methodology is highly modular and compatible with conventional patterning and microfabrication techniques for production of functional biosensing substrates. Furthermore the described combination

of specific bioenabled immobilization technology with functional ferroelectric substrates opens a path to fabricate protein self-assemblies with arbitrary designs for applications in tunable catch-and-release biosensor systems. The bioenabled self-assembly technology additionally provides improved outcomes over the conventional synthetic techniques since the peptide-based tags can concurrently direct, control, and enhance protein immobilization onto defined and specific solid surfaces in a relatively simple process while under biologically and environmentally friendly conditions. Engineered peptides provide promising biological routes for fabrication of inorganic materials with programmable and well-defined biological and inorganic interfaces.

EXPERIMENTAL SECTION

The silver-binding peptides were selected from FliTrx bacterial surface library (Invitrogen, USA) displaying randomized dodecapeptides inserted into FLITRX chimera bacterial surface flagellin protein. The binding affinities of the 50 isolated clones were further characterized by fluorescence microscopy (FM).[29] Selected silver-binding peptides (AgBP1C and AgBP2C) were synthesized using standard Fmoc Solid-phase peptide synthesis and purified using HLPC (Bio-Peptide Co., USA).

Recombinant *E. coli* strain ER2507 bacteria harboring MBP-GFPuv and MBP-GFPuv-AgBP2C plasmid constructs were grown in LB medium. The expression of MBP-GFPuv-AgBP2C was induced by adding IPTG (isopropyl-beta-D-thiogalactopyranoside) at OD_{600} of 0.6 to a final concentration of 0.3 mM. The expressed protein was purified on an amylose resin column (New England Biolabs, USA) and analyzed by 12% SDS–PAGE. Detailed description of cloning and expression protocols is given in the Supporting Information.

SPR measurements were performed using a four-channel instrument (Kretschmann configuration) developed by the Radio Engineering Institute, Czech Republic. The degassed peptide solutions in phosphate buffer at 0.66 μM were flowed over the Ag or Au surface and peptide adsorption kinetics were monitored. After the surface coverage reached or neared equilibrium, the phosphate buffer solution was flowed again and desorption of the peptide was monitored. For data analysis purposes, the SPR signal was calibrated in order to calculate molecules per cm^2 from the surface plasmon wavelength given by the raw data.[33] Detailed description of adhered peptide mass calculations is provided in the Supporting Information.

MBP-GFP-AgBP2C constructs and MBP-GFPuv (8 μM) were incubated on clean PDMS stamps for 10 min. Excess protein was then removed and the stamps were gently dried with nitrogen. The clean silver surfaces were placed in contact with the protein-loaded stamps, incubated for 10 min, removed, washed with DI water, and dried with nitrogen. The MBP-GFPuv-AgBP2C fusion protein arrays were imaged using a fluorescence microscope (Nikon, Japan) and FITC filter (FM).

The PPLN substrate was irradiated by a 313 nm UV light for 20 min right above 10 mM $AgNO_3$ solution at room temperature using UV spot light source (Hamamatsu 5662, Japan) equipped with a 200 W mercury–xenon lamp. After irradiation, the substrate was rinsed in deionized water and then blown dry with nitrogen. The PPLN substrate was irradiated with UV light for a constant period of time to minimize the morphological variations due to the photochemical deposition conditions effect on the AgNP size.[25,26]

MBP-GFPuv-AgBP2C and MBP-GFPuv proteins (50 μM) were drop incubated on the patterned surface for 2 h in a humidified chamber to prevent evaporation. The protein-patterned surface was gently washed for 1 min with DI water, dried with nitrogen, and imaged using FM as described above. The protein bound on the AgNPs patterned surface was analyzed on Raman spectroscopy carried out using a Renishaw InVia Raman spectrometer attached to a Leica DMLM upright microscope.

ASSOCIATED CONTENT

Supporting Information

Detailed experimental procedures, additional surface plasmon resonance, and fluorescence microscopy results (PDF). This material is available free of charge via the Internet at http://pubs.acs.org.

AUTHOR INFORMATION

Corresponding Author

*Telephone: 206-616-6980. Fax: 206-543-3100. E-mail: candan@u.washington.edu.

Author Contributions

‡These authors contributed equally to this work.

Notes

The authors declare no competing financial interest.

ACKNOWLEDGMENTS

This work was supported by grants from the National Science Foundation through the NSF-MRSEC Program (DMR 0520567) at the Genetically Engineered Materials Science and Engineering Center (GEMSEC), TUBITAK/NSF-IRES joint project, NSF (DMR-0706655) through BMAT program at the University of Washington, as well as by the World Premier Institute Initiative for Materials Nanoarchitectonics (MANA) in the National Institute for Materials Science, Japan. The PDMS stamps were prepared at the UW NanoTech User Facility (NTUF). The authors thank James Park for technical help with Surface Plasmon Resonance. The authors are grateful for the comments provided by Prof. Mehmet Sarikaya throughout the work. X.L. also acknowledges Prof. J. Li for AFM facility support. The Asylum Research MFP-3D AFM was acquired through an ARO DURIP grant (W911NF-08-01-0262).

REFERENCES

(1) Qin, D.; Xia, Y. N.; Whitesides, G. M. *Nat. Protoc.* **2010**, *5*, 491–502.
(2) Hammond, P. T. *Adv. Mater.* **2004**, *16*, 1271–1293.
(3) Seo, H. S.; Kim, S. E.; Park, J. S.; Lee, J. H.; Yang, K. Y.; Lee, H.; Lee, K. E.; Han, S. S.; Lee, J. *Adv. Funct. Mater.* **2010**, *20*, 4055–4061.
(4) Tang, Z. Y.; Wang, Y.; Podsiadlo, P.; Kotov, N. A. *Adv. Mater.* **2006**, *18*, 3203–3224.
(5) Anker, J. N.; Hall, W. P.; Lyandres, O.; Shah, N. C.; Zhao, J.; Van Duyne, R. P. *Nat. Mater.* **2008**, *7*, 442–453.
(6) Puurunen, R. L. *J. Appl. Phys.* **2005**, *97*, 52.
(7) Schwartz, D. K.; Garnaes, J.; Viswanathan, R.; Zasadzinski, J. A. N. *Science* **1992**, *257*, 508–511.
(8) Boudou, T.; Crouzier, T.; Ren, K. F.; Blin, G.; Picart, C. *Adv. Mater.* **2010**, *22*, 441–467.
(9) Mrksich, M.; Whitesides, G. M. *Annu. Rev. Biophys. Biomol. Struct.* **1996**, *25*, 55–78.
(10) Kacar, T.; Zin, M. T.; So, C.; Wilson, B.; Ma, H.; Gul-Karaguler, N.; Jen, A. K. Y.; Sarikaya, M.; Tamerler, C. *Biotechnol. Bioeng.* **2009**, *103*, 696–705.
(11) Tamerler, C.; Khatayevich, D.; Gungormus, M.; Kacar, T.; Oren, E. E.; Hnilova, M.; Sarikaya, M. *Biopolymers* **2010**, *94*, 78–94.

(12) Krauland, E. M.; Peelle, B. R.; Wittrup, K. D.; Belcher, A. M. *Biotechnol. Bioeng.* **2007**, *97*, 1009−1020.
(13) Whaley, S. R.; English, D. S.; Hu, E. L.; Barbara, P. F.; Belcher, A. M. *Nature* **2000**, *405*, 665−668.
(14) Sarikaya, M.; Tamerler, C.; Jen, A. K. Y.; Schulten, K.; Baneyx, F. *Nat. Mater.* **2003**, *2*, 577−585.
(15) Evans, J. S.; Samudrala, R.; Walsh, T. R.; Oren, E. E.; Tamerler, C. *MRS Bull.* **2008**, *33*, 514−518.
(16) Dai, H. X.; Choe, W. S.; Thai, C. K.; Sarikaya, M.; Traxler, B. A.; Baneyx, F.; Schwartz, D. T. *J. Am. Chem. Soc.* **2005**, *127*, 15637−15643.
(17) Sengupta, A.; Thai, C. K.; Sastry, M. S. R.; Matthaei, J. F.; Schwartz, D. T.; Davis, E. J.; Baneyx, F. *Langmuir* **2008**, *24*, 2000−2008.
(18) Khatayevich, D.; Gungormus, M.; Yazici, H.; So, C.; Cetinel, S.; Ma, H.; Jen, A.; Tamerler, C.; Sarikaya, M. *Acta Biomater.* **2010**, *6*, 4634−4641.
(19) Hnilova, M.; Khatayevich, D.; Carlson, A.; Oren, E. E.; Gresswell, C.; Zheng, S.; Ohuchi, F.; Sarikaya, M.; Tamerler, C. *J. Colloid Interface Sci.* **2012**, *365*, 97−102.
(20) Yuca, E.; Karatas, A. Y.; Seker, U. O. S.; Gungormus, M.; Dinler-Doganay, G.; Sarikaya, M.; Tamerler, C. *Biotechnol. Bioeng.* **2011**, *108*, 1021−1030.
(21) Kumara, M. T.; Tripp, B. C.; Muralidharan, S. *Chem. Mater.* **2007**, *19*, 2056−2064.
(22) Park, T. J.; Zheng, S.; Kang, Y. J.; Lee, S. Y. *FEMS Microbiol. Lett.* **2009**, *293*, 141−147.
(23) Zheng, S.; Kim, D. K.; Park, T. J.; Lee, S. J.; Lee, S. Y. *Talanta* **2010**, *82*, 803−809.
(24) Slocik, J. M.; Naik, R. R.; Stone, M. O.; Wright, D. W. *J. Mater. Chem.* **2005**, *15*, 749−753.
(25) Kalinin, S. V.; Bonnell, D. A.; Alvarez, T.; Lei, X. J.; Hu, Z. H.; Shao, R.; Ferris, J. H. *Adv. Mater.* **2004**, *16*, 795-+.
(26) Liu, X.; Kitamura, K.; Terabe, K.; Hatano, H.; Ohashi, N. *Appl. Phys. Lett.* **2007**, *91*, 3.
(27) Haussmann, A.; Milde, P.; Erler, C.; Eng, L. M. *Nano Lett.* **2009**, *9*, 763−768.
(28) Lu, Z. J.; Murray, K. S.; Vancleave, V.; Lavallie, E. R.; Stahl, M. L.; McCoy, J. M. *Bio-Technology* **1995**, *13*, 366−372.
(29) Hnilova, M.; Oren, E. E.; Seker, U. O. S.; Wilson, B. R.; Collino, S.; Evans, J. S.; Tamerler, C.; Sarikaya, M. *Langmuir* **2008**, *24*, 12440−12445.
(30) Porter, M. D.; Bright, T. B.; Allara, D. L.; Chidsey, C. E. D. *J. Am. Chem. Soc.* **1987**, *109*, 3559−3568.
(31) Love, J. C.; Estroff, L. A.; Kriebel, J. K.; Nuzzo, R. G.; Whitesides, G. M. *Chem. Rev.* **2005**, *105*, 1103−1169.
(32) Tamerler, C.; Oren, E. E.; Duman, M.; Venkatasubramanian, E.; Sarikaya, M. *Langmuir* **2006**, *22*, 7712−7718.
(33) Jung, L. S.; Campbell, C. T.; Chinowsky, T. M.; Mar, M. N.; Yee, S. S. *Langmuir* **1998**, *14*, 5636−5648.
(34) Tamerler, C.; Duman, M.; Oren, E. E.; Gungormus, M.; Xiong, X. R.; Kacar, T.; Parviz, B. A.; Sarikaya, M. *Small* **2006**, *2*, 1372−1378.
(35) Kacar, T.; Ray, J.; Gungormus, M.; Oren, E. E.; Tamerler, C.; Sarikaya, M. *Adv. Mater.* **2009**, *21*, 295−299.
(36) Oren, E. E.; Tamerler, C.; Sahin, D.; Hnilova, M.; Seker, U. O. S.; Sarikaya, M.; Samudrala, R. *Bioinformatics* **2007**, *23*, 2816−2822.
(37) Myers, L. E.; Miller, G. D.; Eckardt, R. C.; Fejer, M. M.; Byer, R. L. *Opt. Lett.* **1995**, *20*, 52−54.
(38) Kim, S.; Gopalan, V.; Kitamura, K.; Furukawa, Y. *J. Appl. Phys.* **2001**, *90*, 2949−2963.
(39) Liu, X. Y.; Ohuchi, F.; Kitamura, K. *Funct. Mater. Lett.* **2008**, *1*, 177−182.
(40) Barth, A. *Prog. Biophys. Mol. Biol.* **2000**, *74*, 141−173.
(41) Scott, J. G.; Mailis, S.; Sones, C. L.; Eason, R. W. *Appl. Phys. A: Mater. Sci. Process.* **2004**, *79*, 691−696.